THE DESIGN OF A HIGH POWER GYROKLYSTRON FOR SUPERCOLLIDER APPLICATIONS*

W. Lawson, J. Calame, V. L. Granatstein, P. E. Latham,
M. E. Read,[a] C. D. Striffler, W. Wang, D. Welsh, and F. J. Williams

Electrical Engineering Department
and
Laboratory for Plasma and Fusion Energy Studies
University of Maryland, College Park, MD 20742

Abstract

In this paper, we focus on the theoretical and experimental design of a 30-50 MW peak power, X-band gyroklystron. We discuss the theoretical tools and designs for the electron gun and microwave circuit. We predict ~ 45% efficiency and ~ 63 dB gain in the TE^{o}_{01} mode using a 500 kV, 160 A beam. Pulse duration will be in the range 1-2 μs. Cold test results of the microwave circuit are presented along with the experimental characteristics of the modulator.

Introduction

The practical development of linear supercolliders may require high frequency (~ 10 GHz) and high peak power (~ 200 MW) microwave sources with a pulse duration of ~ 135 ns. One promising candiate is the gyroklystron, which has the potential to achieve these specifications with the necessary gain, efficiency, and stability [1-2]. The University of Maryland's gyroklystron experiment, which is currently under construction, is shown schematically in Fig. 1. The nominal operating parameters are listed in Table I. A line-type modulator provides the required voltage pulse and the annular, spiraling beam is produced by a thermionic double anode Magnetron Injection Gun (MIG). The beam interacts with the microwave circuit, which consists of four right circular cavities separated by drift sections, and is collected in the beam dump. The input cavity is driven in the lowest circular electric mode, the two intermediate cavities enhance beam bunching and gain, and the output cavity has a coupling iris for energy extraction.

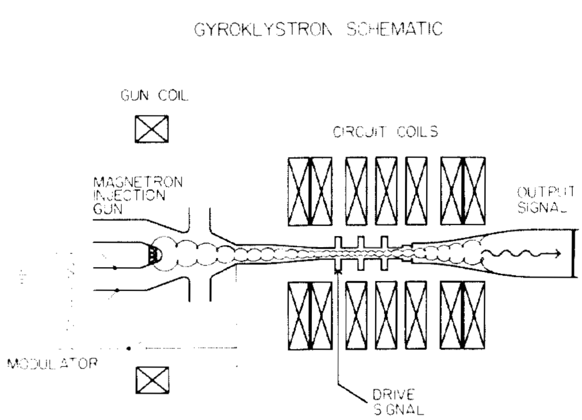

FIG. 1. The University of Maryland gyroklystron.

Details of the three major subsystems (modulator, electron gun, and microwave circuit) will be discussed below. Other experimental hardware, including the beam dump, output window, and diagnostic systems, will also be mentioned.

Table I. The beam parameters.

Beam Power P_o	80 MW
Beam Voltage V_o	500 kV
Magnetic Field B_o	0.555 T
Velocity Ratio $v_\perp/v_z$	1.5
Guiding Center Radius r_g	0.79 cm
Larmor Radius r_L	0.43 cm

The Modulator

A simplified modulator schematic is shown in Fig. 2. Four pulse-forming networks (PFN's) in parallel are resonantly charged to 46 kV using a 0.68 H charging inductor. This charging cycle is triggered using a spark gap, and derives its energy from a 10 μF storage bank. The bank is continually recharged to 25 kV from the main power supply at approximately 180 mA. Shot-to-shot voltage regulation of better than 1% is achieved by interrupting the charging cycle when the PFN voltage has reached a suitable level. To accomplish this, an SCR connects a small resistance to a low voltage secondary winding on the charging inductor. The PFN's have 8-12 stages to provide pulses of 1-2 μs. While the PFN capacitors are fixed at 0.014 μF, the inductors can be varied between 0.5 and 3.5 μH by choosing a suitable tap point and by inserting a copper tuning slug. The PFN's are switched through two thyratrons into a 1:22 pulse transformer which provides the required potential of 500 kV and current of 400 A. Approximately half of the available current is shunted through a compensated resistive divider to provide an intermediate voltage for a modulation anode in the electron gun.

A simplified modulator with resistive charging, a spark gap trigger, and a purely resistive load has been tested. This configuration was capable of demonstrating all the modulator requirements except for repetition rate and shot-to-shot repeatability. Successful operation at 500 keV, 400 A was achieved with 1.5 μs flat-top pulses. A typical experimental output trace is shown in Fig 3. A flat-top ripple of less than 1% was achieved with inductance tuning and a simple loading network.

*Supported by the U.S. Department of Energy.
a) Physical Sciences, Inc. Alexandria, VA.

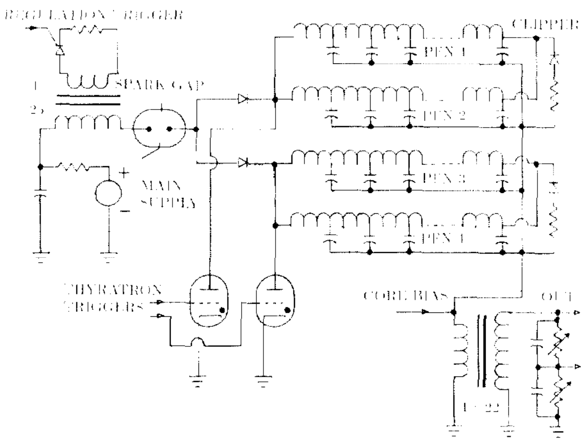

FIG. 2. A simplified modulator schematic.

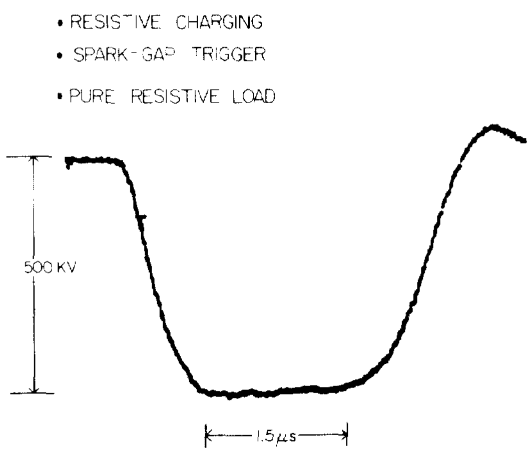

FIG. 3. A typical modulator output pulse.

The Magnetron Injection Gun

The electrode configuration for the double-anode MIG is shown in Fig. 4 and the electrode specifications are listed in Table II. The velocity ratio of $\alpha = v_{\perp}/v_z = 1.5$ is required to achieve a lab frame efficiency of > 40%. For a 160 A beam, the selected cathode radius achieves a cathode loading which is 40% of the electron gun's space-charge limited current while maintaining peak electric fields below 90 kV/cm on all surfaces. The magnetic field is generated by a set of seven water-cooled pancake coils in the microwave circuit region and supplemented by a gun coil over the cathode. The pancake coils have a 15 cm diameter bore and carry ≈ 450 A. The total magnetic compression of 12 occurs in the 48 cm region between the emitter strip center and the entrance to the microwave circuit. Electron motion in the MIG has been simulated by a fixed mesh code at the University of Maryland and a variable mesh code at Varian [3]. The current capability of the MIG is illustrated in Fig. 5. Both simulations anticipate operation under 10% axial velocity spread from 120 A to 240 A. The minimum spread of 6.4% occurs at the nominal operating current of 160 A.

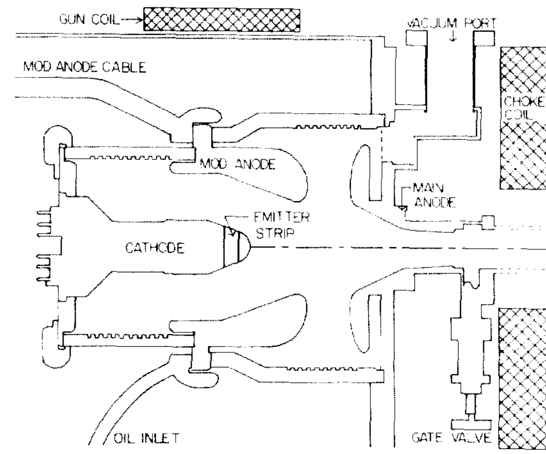

FIG. 4. The magnetron injection gun.

Table II. The electrode specifications.

Average Cathode Radius r_c	2.3 cm
Cathode-Mod Anode Gap d_{ac}	6.1 cm
Cathode Half-Angle ϕ_c	20^0
Magnetic Compression B_o/B_c	12
Mod Anode Voltage V_a	143 kV
Cathode Loading J_c (160 A)	5.6 A/cm^2

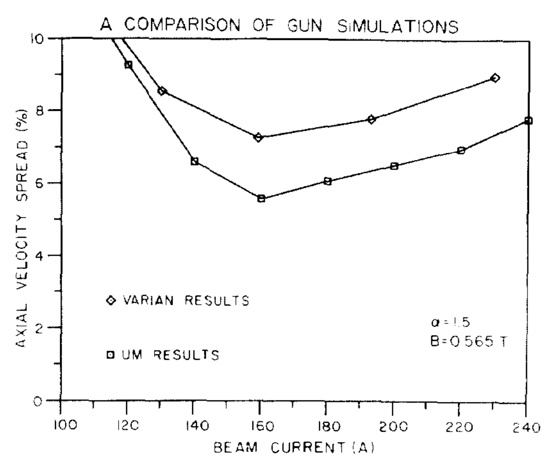

FIG. 5. The range of operating currents.

The Gyroklystron Circuit

The design for the gyroklystron circuit is shown in Fig. 6(a) and the relevant dimensions are listed in Table III. The optimized design is found with the aid of a partially self-consistent steady-state code [4] that uses the beam parameters from the gun simulation. Particle trajectories are numerically integrated through the cold cavity electromagnetic fields, which consist of only circular electric (TE^{0}_{on}) modes. The relative amplitudes of the circular harmonics are computed using a mode expansion in the cavities and drift tubes. The cavity Q's are such that 160 A is 75% of the start oscillation current in the input and buncher cavities and 101% of the start oscillation current in the output cavity. Detuning the final two cavities enhances efficiency at the expense of gain.

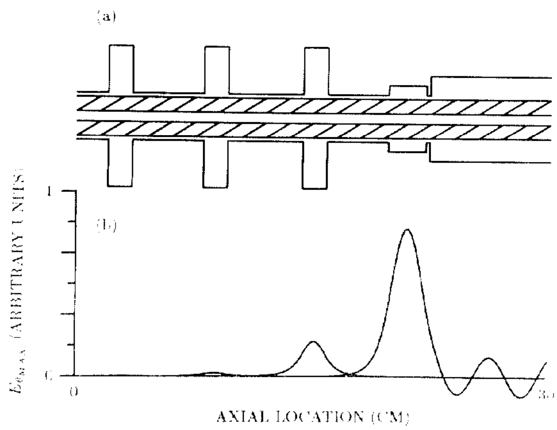

FIG. 6. The gyroklystron circuit: (a) conductor geometry and (b) azimuthal electric field.

Table III. Optimized gyroklystron circuit dimensions.

Cavity No.	Q	f_{res} (GHz)	Length (cm)	Radius (cm)
1	235	10.000	1.53	4.50
2	235	10.000	1.53	4.50
3	240	9.975	1.53	4.50
4	180	9.995	2.38	2.11
Drift Tube				
1			4.50	1.50
2			5.40	1.50
3			3.90	1.50
Coupling Iris			0.336	1.50

Figure 6(b) displays the maximum E_θ at the beam center as a function of position in the microwave circuit. The phase shift between cavities is not indicated in the figure. The electric field in the first cavity is too small to be seen; the alternating field to the right of the fourth cavity represents the outgoing wave of the endfire system. Although the field amplitudes decrease rapidly in the drift regions, indicating adequate isolation between cavities, the finite drift tube fields drastically affect circuit performance. Contour plots of saturated efficiency as a function of B_o and $\Delta v_z/v_z$ are displayed in Fig. 7. In a perfectly cold beam with no velocity spread, the predicted optimum efficiency is ~ 50%. This falls to 45.5% when $\Delta v_z/v_z$ = 6.4%, because the spread in velocity prevents tight phase bunching of the electrons. This deleterious effect of velocity spread was minimized in the design by keeping the drift tubes short, which required relatively large cavity fields. The corresponding large-signal gain is ~ 63 dB.

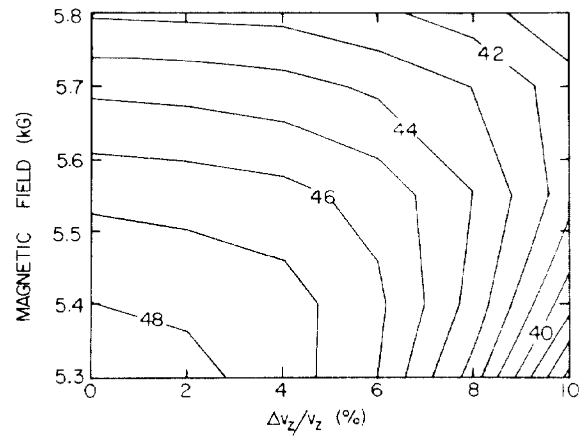

FIG. 7. Contour plot of saturated efficiency on the (B_o, Δv_z) plane.

The output cavity Q is essentially diffractive and is sufficiently larger than the minimum Q so that a simple coupling iris can be used for the endfire system. Cold testing has confirmed both the frequency and Q predicted by the mode expansion code. The Q's of the input and buncher cavities are resistive; a cavity with a ring of carbon-impregnated alumino-silicate placed against the outer wall, approximately 3 mm thick on one side and tapered to a knife edge on the other, achieved the desired Q in cold-testing. Microwave power is injected into the input cavity through a resonant coupler.

Experimental Hardware

A short taper connects the coupling iris of the output cavity to the water cooled, stainless steel beam dump. The taper is nonlinear to minimize mode conversion of the microwave signal. The beam dump radius is 3.81 cm and its length is ~ 35 cm, insuring an instantaneous temperature rise of no more than 20^0 C/pulse. A dumping magnet allows no electrons to pass the beam dump area. A second nonlinear taper takes the waveguide up to the 6.35 cm radius required for the half-wavelength, beryllia output window. A 20 hole, 48 dB directional coupler is used with a diode to sample the output pulse shape and estimate the power. A nonresonant waterload measures the full average power. Rogowski coils and capacitive probes are used together to determine beam current and average velocity ratio.

References

[1] V. L. Granatstein, et al., IEEE Trans. Nucl. Sci. NS-32, 2957 (1985).
[2] W. Lawson, et al., 1986 IEDM Tech. Digest, p. 334.
[3] W. Lawson, et al., Int. J. Electron. 61, 969 (1986).
[4] K. R. Chu, et al., IEEE Trans. Plasma Sci. PS-13, 417 (1985).
[5] J. M. Baird and W. Lawson, Int. J. Electron. 61, 953 (1986).